Visual Abstract

Modelling of fresh properties and strength activity index with microstructure characterisation of ternary cement incorporating waste glass and granulated blast furnace slag

Salah Eddine Daguiani
Laboratory of Exploitation and Valorisation of Natural Resources in Arid Zones (E.V.R.N.Z.A.), Department of Civil Engineering and Hydraulic, Faculty of Applied Sciences, Kasdi Merbah University of Ouargla, 30000, Algeria
daguiani.salaheddine@univ-ouargla.dz, salahdaguiani@hotmail.com, https://orcid.org/0000-0001-6707-0386

Oussama Kessal
Mohamed El Bachir El Ibrahimi, University of Bordj Bou Arreridj, 34 000, Algeria.
oussama.kessal@univ-bba.dz, https://orcid.org/0000-0002-3669-6164

Abdelouahed Kriker, Abdessamed Mokhtari
Laboratory of Exploitation and Valorisation of Natural Resources in Arid Zones (E.V.R.N.Z.A.), Department of Civil Engineering and Hydraulic, Faculty of Applied Sciences, Kasdi Merbah University of Ouargla, 30000, Algeria
a_kriker@yahoo.fr, https://orcid.org/0000-0003-2417-2942
mokh_ab70@yahoo.fr

ABSTRACT. Research in innovative construction materials has focused on utilising supplementary materials in cementitious composites to promote sustainable development and reduce CO_2 emissions. Within this context, this study aims to investigate the fresh properties and assess the pozzolanic activity of ternary blended cement by incorporating two industrial waste materials, namely waste glass (WG) and granulated blast furnace slag (GBS), as cement replacements up to 30%. A mixture design approach was employed for composition optimisation, and mathematical models were implemented to achieve this. XRD and SEM/EDS analyses were conducted to examine the structure and composition of the cementitious matrix.
The results indicate that the setting time was prolonged compared to the reference mixture. Furthermore, based on the results of the SAI (Strength Activity Index) test, an acceptable level of strength development was demonstrated, confirming that WG and GBS possess the potential to replace cement while meeting the minimum strength requirements outlined in the specifications. Microstructure analyses revealed good adhesion between WGP, GGBS, and the cementitious binder. This research contributes to the development of eco-efficient binders that exhibit increased cement

OPEN ACCESS

Citation: Daguiani, S.E., Kessal, O., Kriker, A., Mokhtari, A., Modeling of fresh properties and strength activity index with microstructure characterization of ternary cement incorporating waste glass and granulated blast furnace slag, Frattura ed Integrità Strutturale, 66 (2023) 88-111.

Received: 21.02.2023
Accepted: 30.07.2023
Online first: 03.08.2023
Published: 01.10.2023

replacement ratios and qualities comparable to, or even superior to, traditional cement systems.

KEYWORDS. Mineral additions, Mixture design approach, Ternary binder, Fresh properties, Microstructure, Strength-activity index.

INTRODUCTION

The world produces a significant quantity of construction materials annually, and this production has increased due to rapid urbanisation and the expanding global population. Cement, since its invention, has been recognised as the most commonly used binding agent in construction materials. Its utilisation has enabled the construction of extensive infrastructure that exhibits high levels of strength and durability at a relatively affordable cost. In Algeria, the annual cement production reaches 18 million tonnes, with a market demand that exceeds this quantity by approximately 5 million tons. This highlights the need to bridge the gap in order to meet the growing market requirements [1]. Cement production is predicted to expand by up to 4 billion tonnes annually by 2030 [2]. Furthermore, its production contributes to nearly 5 to 7 % of carbon dioxide (CO_2) emissions, total global gas emissions [3]. Due to the development of the sector of cement as well as the demand for bolder and slender constructions, ordinary concrete no longer meets the requirements for the execution of these works. In this context, other cementitious mixtures and concretes with properties superior to ordinary concrete evolved to fulfil this need. This is the case for self-compacting, geopolymer, high-performance, high-strength, and, more newly, ultra-high-performance concrete. Supplementary cementitious materials (SCMs) from industrial wastes or natural resources are considered sustainable solutions that can be replaced partially with cement for producing these concretes to achieve better engineering properties and improve performance of these concretes. Several industrial wastes have been successfully used as SCMs, including fly ash, waste glass, marble waste, cement kiln dust, and granulated blast furnace slag [4–7]. Partially replacing cement with these waste materials has both ecological and economic impacts, offering a sustainable and environmentally friendly solution that conserves natural resources [8]. Among these added wastes, granulated blast furnace slag (GBS) is a by-product generated from the production of iron and steel, which is removed from the blast furnace in steam or water, dried, transformed into granules, and processed into a powder in a ball mill. GBS is finely ground to produce a product known as ground granulated blast furnace slag (GGBS) [9]. GGBS was used as a cement replacement in the production of concrete from a low amount (10 % - 30 %) [10] to a high amount (50 % - 80 %) [4][11]. Crossin, E. [12] has demonstrated that using GGBS as a cement replacement reduced greenhouse gas emissions. According to prior studies, increasing GGBS content in the binder causes lower heat of hydration [13–15]. At high-level replacement of GGBS in binders, the setting time can be slightly extended due to its latent hydraulic properties. Hooton [16] found that the setting time of the GGBS mix can be extended in the range of 60-120 min with low ambient temperature and high replacement levels. The finishing time can only increase by a few minutes in hot weather with temperatures over (20 °C). It makes concrete more workable for extended periods, resulting in fewer joints. Additionally, it is beneficial when applied in warm weather. Other studies [13][17] have shown that mortars with 50 % of slag as a cement substitute are more workable. Rahman et al. reported that using GGBS has no adverse effect on the expansion due to the less free lime available in the mixtures that incorporate GGBS as a cement substitute [18]. Another waste product that is produced in significant amounts and is challenging to get rid of is waste glass (WG). It is well known that WG generates several environmental problems due to its non-biodegradable characteristics. In Algeria, about 170,000 tonnes of glass are discarded annually, even though it takes at least 4000 years to disintegrate [19]. It is called waste glass powder (WGP) when waste glass is finely ground into powder. This waste product is classified as a pozzolanic material since it contains amorphous structures and a significant quantity of calcium and silicon. According to ASTM C 618-12a, it satisfies all of the requirements for pozzolanic materials [20]. Thus, waste glass can be used to replace cement partially. Aliabdo et al. [21] reported that using WGP as cement substituting decreases the water demand. In contrast, when the replacement level of WGP increases, the value of water requirement percentage decreases linearly. In previous studies, it was found that increasing quantities of WGP extended the initial and final setting times of the cement paste [21–23], resulting in better workability [24] as well as higher resistance to chloride penetration of mortar [25].

A synergistic effect may be created by combining different SCMs, which contributes to improved mechanical properties or durability of concrete compared to using it alone [26–28]. Several authors have performed the optimisation of ternary or quaternary cement constituent proportions [26][29–32]. Hence, a few research have been published on optimising the

ternary cement constituent proportions of PC-GGBS-WGP [33]. Additionally, it was noted that the durability aspects and mechanical properties of GGBS mortar or concrete that contained WGP had improved [33–35]. Moreover, different statistical modelling techniques have been extensively used to determine the relative relevance of various mixing factors and examine their combined impacts on important concrete characteristics [36]. The mixture design currently provides a basic test program that assists in empirically modelling the responses [37,38].

Numerous studies have examined the performance and durability of concrete and mortars containing waste glass powder (WGP) and ground granulated blast furnace slag (GGBS) in binary composites. However, it is crucial to acknowledge that grinding slag is a complex and energy-intensive process, while a high glass content in cement can contribute to the alkali-silica reaction. Nevertheless, the combination of these waste materials can yield positive effects on economic and sustainable development. Therefore, this research aims to evaluate the properties of ternary cement by varying the proportions of waste glass powder and ground granulated blast furnace slag as partial replacements for cement. Incorporating these waste materials follows the principles of the 3R's (Recycle, Reuse, Reduce) and allows for a maximum replacement of 30% of cement. The study focuses on assessing key properties of fresh and hardened paste and mortar samples using predictive models generated through the innovative mixture design approach. Fresh properties, such as normal consistency, setting times, and soundness, are determined to understand the behavior of the materials. Hardened properties are evaluated through the strength activity index at 7 and 28 days, comparing the pozzolanic activity of the materials with a reference mixture consisting solely of Portland cement (CEM I 42.5 R). Microstructural investigations utilising techniques such as X-ray diffraction (XRD), scanning electron microscopy (SEM), and energy-dispersive X-ray spectroscopy (EDS) provide insights into the reaction products and engineering characteristics of the pastes.

The findings of this research can serve as valuable guidelines for researchers and manufacturers, facilitating more effective development and utilization of these waste materials in future studies. By implementing these formulations, advancements can be made in achieving sustainable and eco-friendly practices.

Experimental procedure

Materials

A Portland cement (PC) type CEM I-42.5 R provided by Biskria Cement Company (Biskra, Algeria), meeting the European standard EN 197-1, was used. The chemical and physical properties of used cement are summarised in Tab. 1. Two by-products were chosen for cement substitution: waste glass (WG) and granulated blast furnace slag (GBS).WG was brought from a local glass factory, while GBS was obtained from the El-Hadjar steel plant. WG was thoroughly washed afterward to remove unwanted or organic materials, dried, and crushed into tiny pieces (≤ 50 mm). Waste glass powder (WGP) and ground granulated blast furnace slag (GGBS) were sieved through an 80 μm sieve after being ground in a laboratory mill for an approximate grinding time of 60 min. Blaine air permeability apparatus was used for measuring their specific surface area according to the standard ASTM C204-11. They were equal to 4470 and 4640 cm2/g, respectively. Figs. 1 and 2 illustrate WGP and GGBS samples before and after grinding.

(a) (b)

Figure 1: WGP samples before (a) and after (b) grinding.

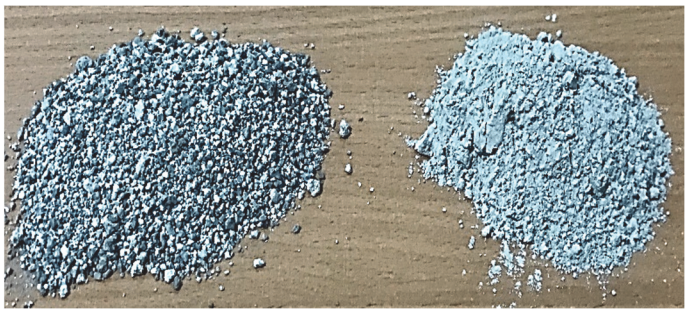

(a) (b)

Figure 2: GGBS samples before (a) and after (b) grinding.

Tab. 1 summarises the chemical characteristics of PC, WGP, and GGBS. They were assessed using a Panalytical PW 2404 X-Ray Fluorescence Spectrometer (XRF). However, it was found that the used by-products are rich in SiO_2, Al_2O_3, Fe_2O_3, and their summation was higher than 70 % for pozzolans, the minimum required following ASTM C 618-12a standard.

Composition of oxides (%)	PC	WGP	GGBS
SiO_2	19.715	69.34	38.968
Al_2O_3	4.973	1.778	6.611
CaO	61.74	9.807	44.255
Fe_2O_3	3.322	0.571	2.545
MgO	3.331	2.299	2.237
SO_3	2.347	0.335	1.266
K_2O	0.653	0.261	0.84
Cl	0.03	0.026	0.011
Na_2O	0.152	12.431	0.181
Loss on ignition (LOI)	2.50	0.40	1.20
Physical properties			
Specific density (g/cm^3)	3.07	2.63	2.90
Specific surface area (cm^2/g)	3320	4470	4640

Table 1: Chemical and physical properties of studied constituents.

Fig. 3 illustrates the mineralogical constitution of the studied cementitious binders, defined by X-ray diffraction (XRD).

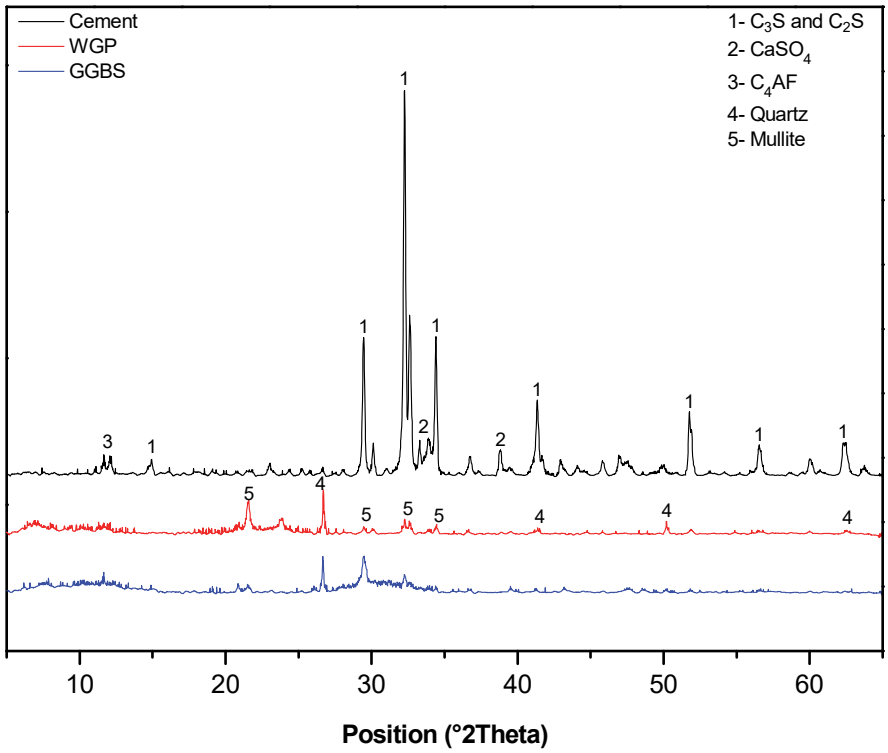

Figure 3: X-ray diffraction (XRD) analysis of studied constituents

The particle size distribution of PC, WGP, and GGBS is shown in Fig. 4.

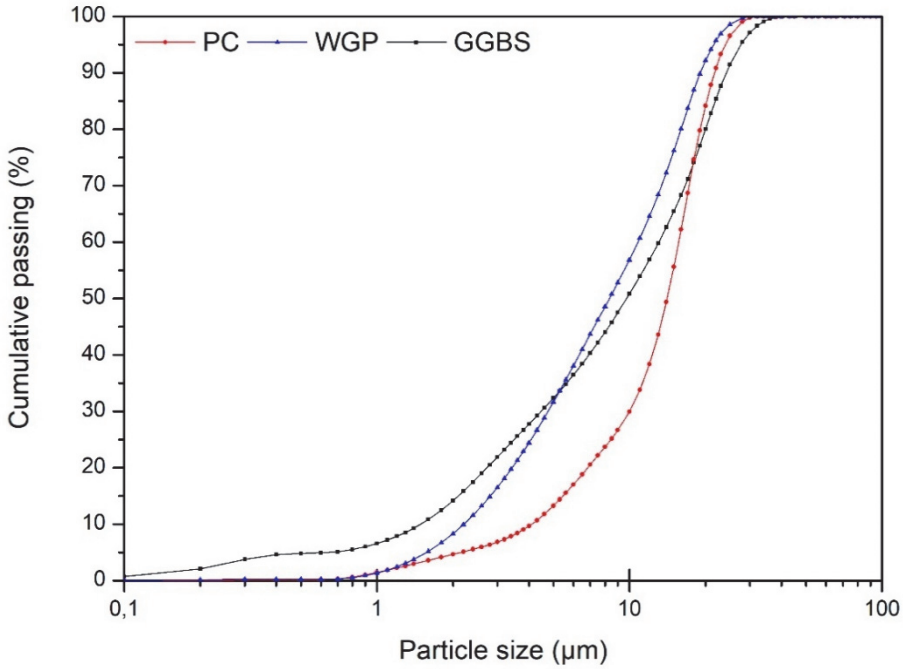

Figure 4: Particle size distribution of studied constituents

Mixture design approach

The mixture design approach is a new technique used when examining products of various components that depend on the effects of different factors and to organise better the experimental tests that support scientific research or industrial studies. It considers the impact of each factor not only separately but also with the interaction between several factors, which are the proportions of each component (X_i) of the mixture (proportions of PC, WGP, and GGBS) on the studied responses (Y), which are presented as a function of these proportions (Consistency, setting time, soundness and strength-activity index of the cement sample). Indeed, it allows for a remarkable reduction in the number of experiments and the planning and execution of the research. Using this method will be very interesting for studying the following function type :

$$Y = f(X_i) \tag{1}$$

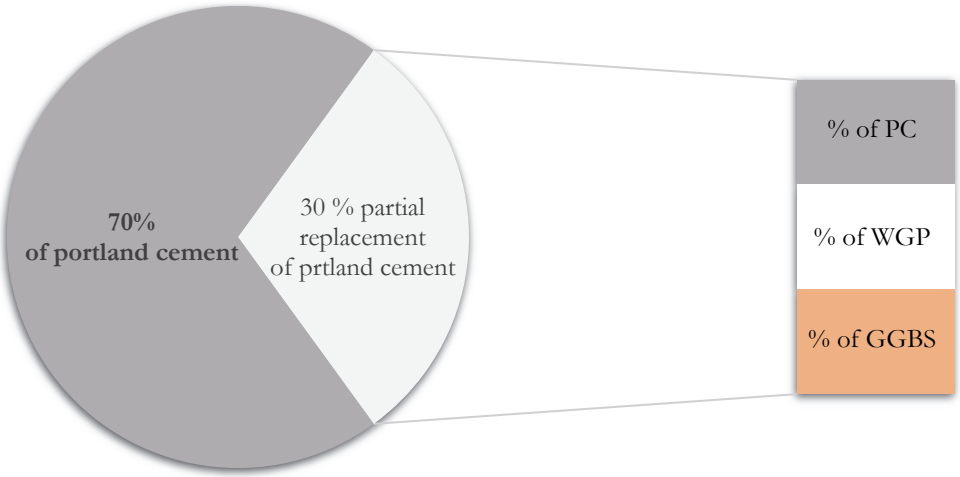

Figure 5: Substitution of cement by mineral additions

The purpose of the present work is to examine the effect of WGP and GGBS on the consistency, initial and final setting time, soundness, and strength-activity index of the cement sample using a mixture design with 03 factors (PC, WGP, and

GGBS) and replacement of 30 % of cement, as shown in Fig. 5. In light of this, we must consider a mixture design with three factors taken in mass proportions (PC %, WGP %, and GGBS %).

Mixture proportions

Understanding the role of the different factors (PC, WGP, and GGBS contents) separately on pastes properties is the goal target of the present work. The Sum of concentrations achieves the following relationship:

$$\%PC + \%WGP + \%GGBS = 100\% \tag{2}$$

The total number of experiments was determined using the following equation:

$$N = \frac{(f + l - 1)!}{(l)!(f - 1)!} \tag{3}$$

where: (*f*) is the number of factors and (*l*) is the number of levels.

The combination number treated was (C=15) based on four levels and three factors to determine the impact of these factors on the characteristics of pastes. The positions of the 15 mixtures on the ternary diagram are depicted in Fig. 6.

The statistical model used to describe the variation of the measured values is a second-degree polynomial in the dependent variables PC, WGP, and GGBS. This model can be expressed in the form :

$$\begin{aligned} Y = {} & X_1 \times (PC) + X_2 \times (WGP) + X_3 \times (GGBS) + X_{12} \times (PC \times WGP) + \\ & + X_{13} \times (PC \times GGBS) + X_{23} \times (WGP \times GGBS) \end{aligned} \tag{4}$$

where: (Y) is the expected response and (X_1, X_2, X_3, X_{12}, X_{13}, X_{23}) are the model coefficients.

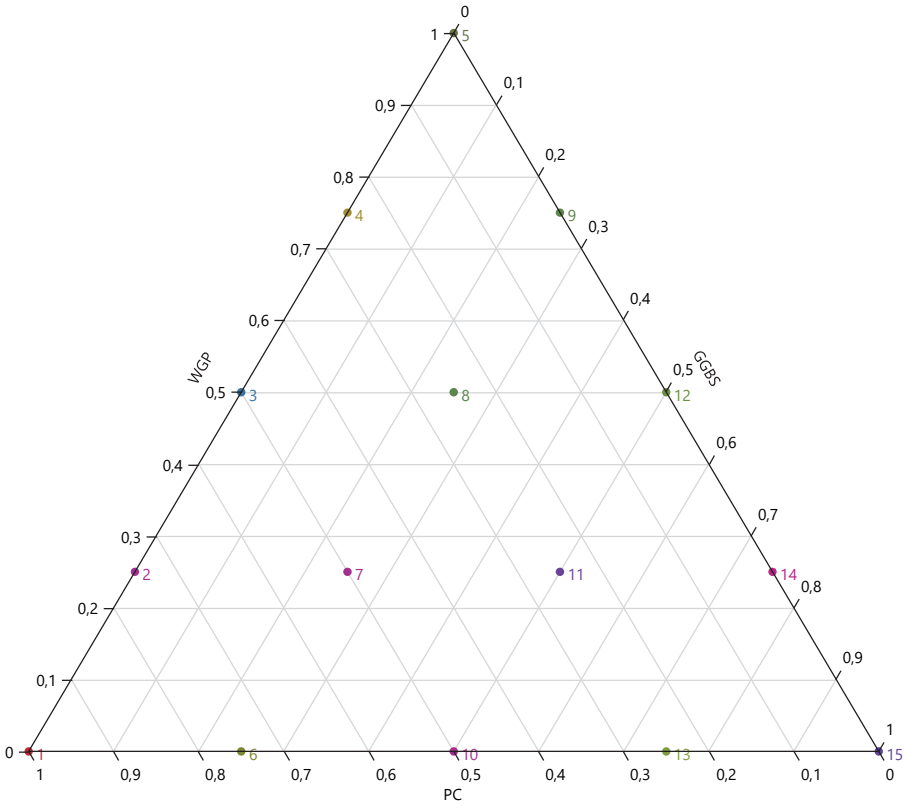

Figure 6: Triangular representation of the 15 mixtures according to PC, WGP, and GGBS dosage.

Sample preparation

This study focuses on (PC, WGP, and GGBS) based binary and ternary types of cement. Fifteen mixtures were prepared using the experimental design method. The ternary diagram in Fig. 6 and Tab. 2 illustrates the different proportions of these studied ternary mixtures. Additions were added by substitution, varying from 0 to 30 %. Cement pastes and mortars containing CEM I 42.5 R were used as a control mixture (100 %).

Mixture N°	PC	WGP	GGBS	Mix proportions of mortars for the S.A.I test		
				PC (kg/m³)	WGP (kg/m³)	GGBS (kg/m³)
1	1	0	0	450	0	0
2	0.75	0.25	0	427,5	22,5	0
3	0.5	0.5	0	405	45	0
4	0.25	0.75	0	382,5	67,5	0
5	0	1	0	360	90	0
6	0.75	0	0.25	427,5	0	22,5
7	0.5	0.25	0.25	405	22,5	22,5
8	0.25	0.5	0.25	382,5	45	22,5
9	0	0.75	0.25	360	67,5	22,5
10	0.5	0	0.5	405	0	45
11	0.25	0.25	0.5	382,5	22,5	45
12	0	0.5	0.5	360	45	45
13	0.25	0	0.75	382,5	0	67,5
14	0	0.25	0.75	360	22,5	67,5
15	0	0	1	360	0	90

Sand/Binder ratio = 3

Water/Binder ratio = 0.5

Table 2: Factor values and different studied mixtures.

Experimental mMethod

Several tests have been done to evaluate the fresh characteristics of cement paste mixed with chosen by-products. The control mixture without Scms was compared to the test results. The experimental methods used in this study include consistency, initial and final setting times, and soundness. Experiments were performed in the laboratory using freshly mixed pastes at 20 ± 02 °C and a minimum relative humidity of 50 %. The strength-activity index (SAI) was also investigated.

Consistency test of cement sample

The consistency of the paste is obtained by varying the proportion of water added until it reaches a satisfactory resistance to penetration. The Consistency experiment has been assessed according to European standard EN 196-3. Initially, We determined the mass of cement paste, and then a series of experiments were performed with various (W/C) ratios. Consistency was measured when the plunger of the Vicat apparatus penetrated the paste. It must give a sinking of (6 ± 3) mm over the base of the Vicat mould. The mass of water that was used to achieve the optimal ratio was noted with an M_L.

Setting time test

The initial setting time can be determined as the interval between adding water to the cement powder and the loss of flowability or plasticity of the paste. In contrast, the final setting time refers to the time needed for the cement paste to attain a specific level of hardness necessary to support some load. An automatic Vicat apparatus (63-L2700/E VICAMATIC-2) was used to predict samples' initial and final setting times following the European standard EN 196-3. As with the older generations, the process for the test has not changed; a needle (or a probe) drops freely into a cement sample at fixed positions and regular intervals. A sensor with 0.1 mm resolution is used for measuring penetration depth. The penetration depth decreases along with the hardening process development. The initial and final setting times are recorded when it meets some thresholds pre-defined by standards.

Soundness test of cement sample

The unsoundness of cement causes a diminution in the volume of cement after hardening or setting. After setting, the cement paste expands, disrupting the hardened mass and creating severe problems concerning the strength and durability of the structure. Le-chatelier apparatus detects cement soundness from excess free lime following the European Norm EN 196-3. The cement paste tested corresponds to the standardised consistency. After 24 hours, the distance (A) between the tips of the needles is measured. Then the gap (B) after heating the mould in boiling water. After cooling, the gap (C) is measured. The stability corresponds to the difference between spacings (C) and (A), expressed in mm.
In this test, the hydration of the cement is accelerated by a heat treatment, which makes it possible to measure any expansion in a short time. The expansion must not exceed 10 mm in the Le Chatelier test for measuring soundness.

Strength-activity index (SAI)

Two main categories of test methods can be used for assessing the pozzolanic activity of any mineral material:

- Direct methods to measure the consumption of calcium hydroxide ($Ca(OH)_2$) with the Saturated lime test or Frattini test.
- The indirect method measures test specimens' relative compressive strength-the Strength activity index (SAI).

In this study, we opted to use the indirect method, i.e., the Strength-activity index method determined in eq. 5 as the proportion between the compressive strength of test mortar with 20 % of mineral addition as cement replacement to that of the reference mortar at a specific age in agreement with ASTM C311/C311M-22 standard.

$$\text{Strength - activity index}(\%) = \frac{\sigma_{st}\left(\text{test mortar cube specimen}\right)}{\sigma_{st}\left(\text{reference mortar cube specimen}\right)} \tag{5}$$

The Portland cement used in this test must have total alkalinity (Na_2O + 0.658 K_2O) not less than 0.50 % nor more than 0.80 % and a minimum compressive strength of 35 Mpa at 28 days. The reference mortar included 500 g of PC, while the test mixture must contain 400 g of PC and 100 g of WGP and GGBS in binary and ternary combinations. 1375 g of standard sand and 242 ml of water were also used. Cube samples of 5 cm sides were prepared and placed for 24 h after casting in a moist room at 23 ± 2 °C. The samples were cured in water saturated with lime after being demoulded until they were subjected to compressive strength tests at 7 and 28 days.

Identification phase by X-Ray diffraction technique

The identification phase was performed using a powerful non-destructive method for characterising crystalline materials called X-Ray Diffraction technique. It offers information on phases, textures, structures, and other structural parameters, such as crystal defects, crystallinity, and average grain size. D8 ADVANCE diffractometer was used to perform the XRD measurements. This instrument was equipped with an LYNXEYE XE-T position-sensitive detector (Brucker-AXS).
The diffraction diagrams were collected in the 2 θ range from 10-100° under Cu-Kα ƛCu = 1.54060, increment 0.010° 2 θ, and a measuring time per step of 38.40 s. In order to conduct a qualitative examination of the phase composition of the powders samples, the X'Pert High Score Plus software has been used.

Microstructure observation by SEM and EDS

Thermo Scientific Axia ChemiSEM Scanning Electron Microscopy equipped with an energy dispersive spectroscopy (EDS) was used to identify the morphological specifics of the paste mixtures prepared from binary and ternary binders. SEM images of the hydrated cement sample were taken after 28 days of curing. Microstructure observation was carried out on the same samples used for XRD to verify the identification of hydrated products.

RESULTS AND DISCUSSION

Table 3 illustrates the results of experimental characterisation tests for fifteen mixtures entered into JMP 16 software to be converted into mathematical models. These models can describe the effects of the type of addition (PC, WGP and GGBS) on the studied tests (consistency, initial and final setting time, soundness, and Strength-activity index). These models simplify the assessment of evaluating the impact of each factor separately and in combination with other factors. The statistical approach based on the calculation of errors from the experimental test and the mathematical model was used to evaluate the validity of the mathematical models. The most appropriate models are those that have higher correlation coefficients.

Mix N°	Consistency (%)	Initial setting time (min)	Final setting time (min)	Soundness (mm)	Mean 7 days strength (MPa)	Mean 28 days strength (MPa)	Strength activity index	
							7 days (%)	28 days (%)
1	27.90	195	329	0.6	41.68	48.47	100	100
2	28.60	191	335	0.5	38.00	47.6	91.18	98.21
3	28.52	193	346	0.5	33.72	43.75	80.90	90.26
4	28.40	197	350	0.5	31.15	41.00	74.74	84.59
5	28.20	205	425	0.1	30.64	38.25	73.51	78.91
6	28.66	190	410	0.5	40.50	53.57	97.17	110.52
7	28.60	198	335	1	37.32	48.50	89.54	100.10
8	28.70	203	348	1	31.74	44.30	76.15	91.40
9	28.70	208	407	0.9	29.61	42.49	71.04	87.66
10	28.60	195	425	0.5	36.89	49.29	88.51	101.70
11	28.80	209	409	0.9	33.81	47.32	81.12	97.63
12	28.68	205	430	1	30.53	46.00	73.25	94.90
13	28.44	204	429	0.5	34.41	48.32	82.56	99.69
14	28.84	215	433	0.8	30.35	46.61	72.82	96.16
15	28.30	207	439	0.4	32.05	47.50	76.90	98

Table 3: Results of experimental tests.

Mathematical models

The correlation coefficients were relatively high, as shown in Tab. 4. It means that a good correlation exists between the findings from the experimental test and the results that the model expected. It is also important to highlight that a regression method based on the least square optimisation criteria was used to determine these coefficients.

Term	Consistency		Initial setting time		Final setting time		Soundness		7-day S.A.I		28-day S.A.I	
	R^2=0.78		R^2=0.83		R^2=0.85		R^2=0.87		R^2=0.97		R^2=0.92	
	Coeff.	**p-value**	**Coeff.**	**p-value**	**Coeff.**	**p-value**	**Coeff.**	**p-value**	**Coef.**	**p-value**	**Coeff.**	**p-value**
X_1 :PC	28.08	<.0001	192.14	<.0001	346.93	<.0001	0.50	0.0012	101.04	<.0001	103.24	<.0001
X_2 :WGP	28.18	<.0001	203.36	<.0001	420.21	<.0001	0.15	0.1918	72.18	<.0001	78.78	<.0001
X_3 :GGBS	28.30	<.0001	209.21	<.0001	444.43	<.0001	0.32	0.0147	75.86	<.0001	96.56	<.0001
X_{12} : PC-WGP	1.62	0.0150	-14.57	0.3239	-237.7	0.012	1.11	0.0374	-18.56	0.0265	-1.40	0.8913
X_{13} : PC-GGBS	1.65	0.0136	-14	0.3422	87.71	0.280	0.66	0.1840	7.71	0.3000	17.30	0.1152
X_{23} : WGP-GGBS	2.22	0.0026	19.43	0.1975	-71.71	0.372	3.37	<.0001	-6.23	0.3974	23.40	0.0427

Table 4: Results of experimental tests.

As indicated in Tab. 4, the models exhibit good correlation coefficients for all examined responses ($R^2 \geq 0.78$). In addition, most responses have acceptable probabilities (P). According to this table, retaining mathematical models for the predicted responses are written as follows:

$$\begin{aligned} &Consistency\ (\%) = 28.08 \times PC + 28.18 \times WGP + 28.30 \times GGBS \\ &+1.62 \times PC \times WGP + 1.65 \times PC \times GGBS + 2.22 \times WGP \times GGBS \end{aligned} \quad (6)$$

$$\begin{aligned} &Initial\ setting\ time\ (\text{min}) = 192.14 \times PC + 203.36 \times WGP + 209.21 \times GGBS \\ &-14.57 \times PC \times WGP - 14 \times PC \times GGBS + 19.43 \times WGP \times GGBS \end{aligned} \quad (7)$$

$$\begin{aligned} &Final\ setting\ time\ (\text{min}) = 346.93 \times PC + 420.21 \times WGP + 444.43 \times GGBS \\ &-237.7 \times PC \times WGP + 87.71 \times PC \times GGBS - 71.71 \times WGP \times GGBS \end{aligned} \quad (8)$$

$$\begin{aligned} &Soundness\ (mm) = 0.50 \times PC + 0.15 \times WGP + 0.32 \times GGBS \\ &+1.11 \times PC \times WGP + 0.66 \times PC \times GGBS + 3.37 \times WGP \times GGBS \end{aligned} \quad (9)$$

$$\begin{aligned} &07\,day\,SAI\ (\%) = 101.04 \times PC + 72.18 \times WGP + 75.86 \times GGBS \\ &-18.56 \times PC \times WGP + 7.71 \times PC \times GGBS - 6.23 \times WGP \times GGBS \end{aligned} \quad (10)$$

$$\begin{aligned} &28\,day\,SAI\ (\%) = 103.24 \times PC + 78.78 \times WGP + 96.56 \times GGBS \\ &-1.40 \times PC \times WGP + 17.30 \times PC \times GGBS + 23.40 \times WGP \times GGBS \end{aligned} \quad (11)$$

Consistency modelling

The consistency of cement paste is the minimum water requirement to start the chemical reaction between cement and water. The model parameters estimates of studied responses (Consistency) are shown in Tab. 4. According to the mathematical model of consistency (eq.6), it is evident that the proportion and the type of the three factors (PC, WGP, and GGBS) and their mixtures influence the consistency of fresh pastes. We can see from the model that it is initially affected by the increase in GGBS dosage, then by the increases in PC and WGP content, and finally by the multiple coupled effects. The studied parameters impact the percentage of consistency value as it is expressed by each parameter's coefficient and gives good consistency values. The correlation curve between the measured results and predicted values of consistency, as well as the calculated residues of consistency as a function of the predicted values of consistency and the iso-response curve, are demonstrated in Figs. 7 (a),(b), and (c), respectively.

According to the results, Fig. 7 (a) indicates that WGP-cement, GGBS-cement, and WGP-GGBS-cement, binary and ternary mixtures require more water to reach their standard consistency level than the control mixture. The obtained consistency values were fairly average (between 28.20 and 28.84 %), while 27.9 % of water was added to reach the normal consistency of the control (reference) mixture. From the test results, each 7.5 % of WGP cement replacement decreases water requirement by 0.5 %. This behaviour might be caused by the coarser particles of WGP than cement particles or the glassy (smooth) surface of waste glass powder grains. This behaviour may enhance the concrete workability at the same mixing water content. Moreover, These results are consistent with those reported by Ali A. Aliabdo [21].

Similarly, when adding slag by the same percentage, the water demand decreases by 0.6 % to reach the normal consistency of the paste. It is attributed to the inert behaviour of GGBS at the initial mixing and its low water absorption properties. Furthermore, when the WGP dosage increased in the ternary blended cement (PC-WGP-GGBS), a decrease in the water requirement of the paste was noticed. The ternary mixtures M 07, M 08, M 09, M 11, M 12, and M 14 give values higher by 0.5 % to 2.5 % than the control mixture. This finding proves that incorporating WGP and GGBS has beneficial effects as cement replacement since they do not negatively affect paste consistency.

Setting time test results

The hydration of C_3S and C_3A affects the standard setting time of Portland cement, which represents the development of hydrate structures and eventually results in compressive strength and the creation of ettringite and CSH gel. Intending to evaluate the impact of GGBS and WGP supplementary cementitious materials, setting time was studied using initial and final setting time tests. As shown in Tab. 4, the model simulated of initial setting time shows a strong regression model with a significant value of the correlation coefficients, i.e., $R^2 = 0.83$. that indicates a reasonable degree of correlation between

the experimental findings and the expected values from models. Based on the statistical model for predicting the initial setting time, it can be observed that the single factor that affects the initial setting time is GGBS, WGP, and PC, respectively. Previous research [39,40] has demonstrated that an increased dosage of GGBS delays the setting time. According to Heikal et al. [41], the excellent dispersion of GGBS particles caused the delay by decelerating the initial hydration rate. Under the action of binary combination, (WGP-GGBS) has the most influence, followed by (PC-WGP), and (PC-GGBS) has a negligible effect on the initial setting time. With the inclusion of WGP and GGBS as cement replacements, the initial setting time increases to 205 min and 207 min at 30 wt% of WGP and GGBS, respectively. In comparison, the reference mixture's initial setting time is 195 min.

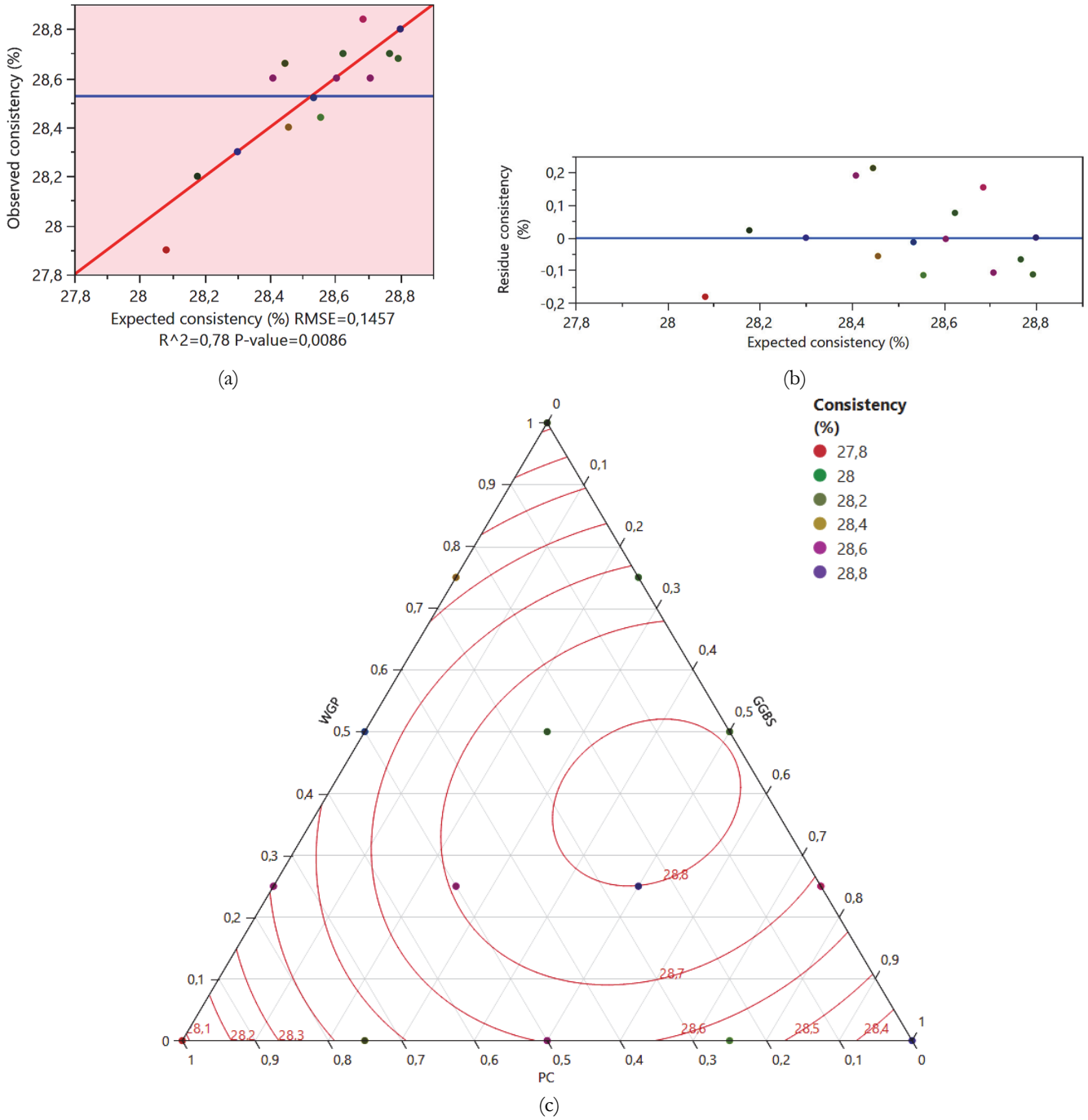

Figure 7: (a) Correlation curve between the observed (experimental) results and the expected results for consistency; (b) Residue vs. expected consistency; (c) Iso-response curve for consistency.

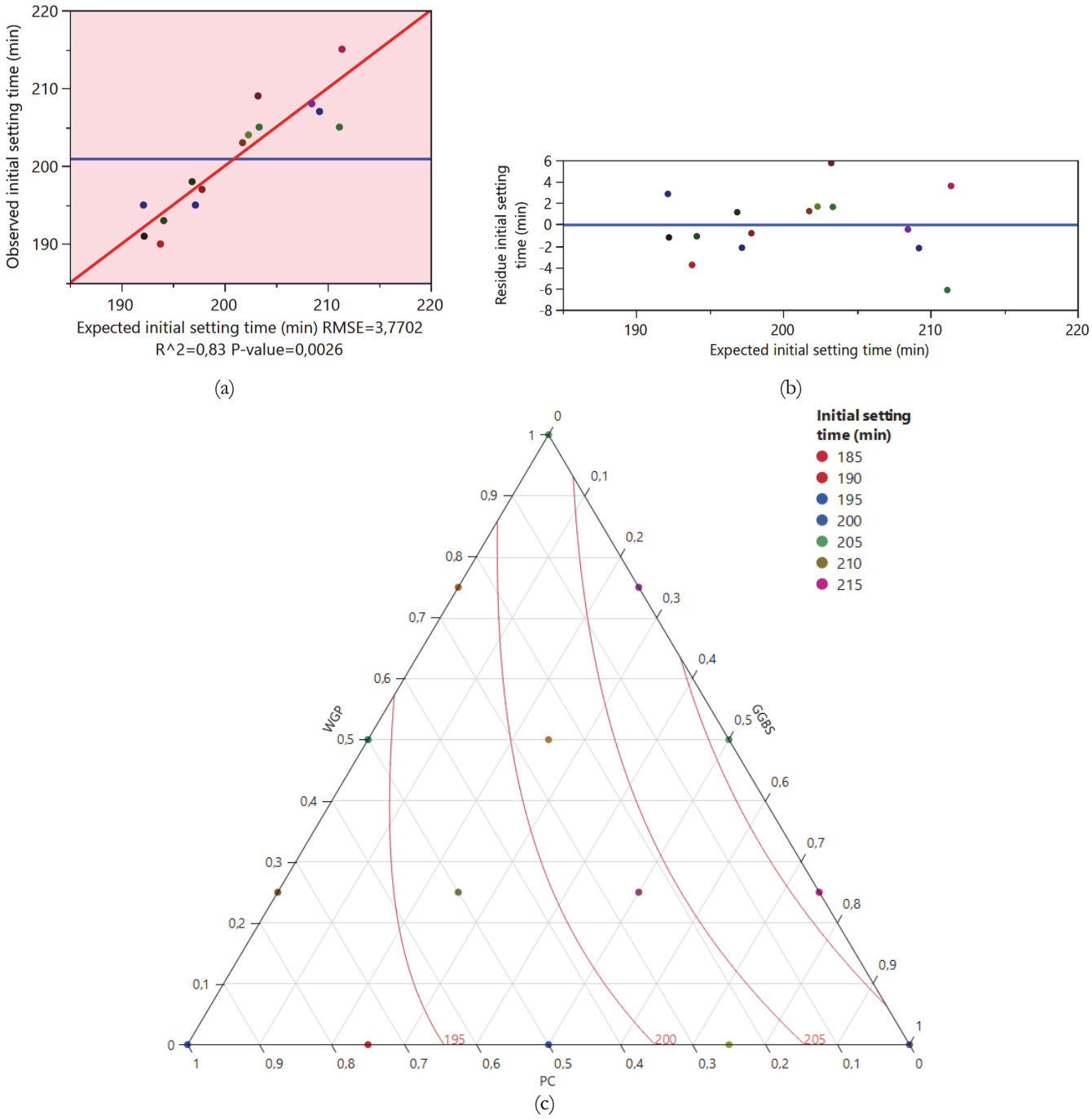

Figure 8: (a) Correlation curve between the observed (experimental) results and the expected results for initial setting time; (b) Residue vs. expected initial setting time; (c) Iso-response curve for initial setting time.

Accordingly, the final setting time increased from 329 min for the control mixture to 425 min and 439 min for 30 % replacement by weight of cement by WGP and GGBS. Since WGP and GGBS replaced the cement, the distribution of the cement grains caused a relatively long setting time and therefore influenced their hydration. Figs. 8 (a), (b), and (c) illustrate, respectively, the Correlation curve between the observed and the expected results for initial setting time, calculated residue as a function of expected initial setting time, and the Iso-response curve for initial setting time. Whereas for the final setting time, the same curves are illustrated in Figs. 9 (a), (b), and (c), respectively. It is obvious that the points are dispersed uniformly along the diagonal, with no outlying points. Additionally, according to the various contents of (PC, WGP, and GGBS), it should be noted that the residues are well dispersed. Furthermore, The results are within the range indicated in ASTM C191-19, which requires that the initial setting time must be at least 60 min and the value of the final setting time should be larger than 90 min.

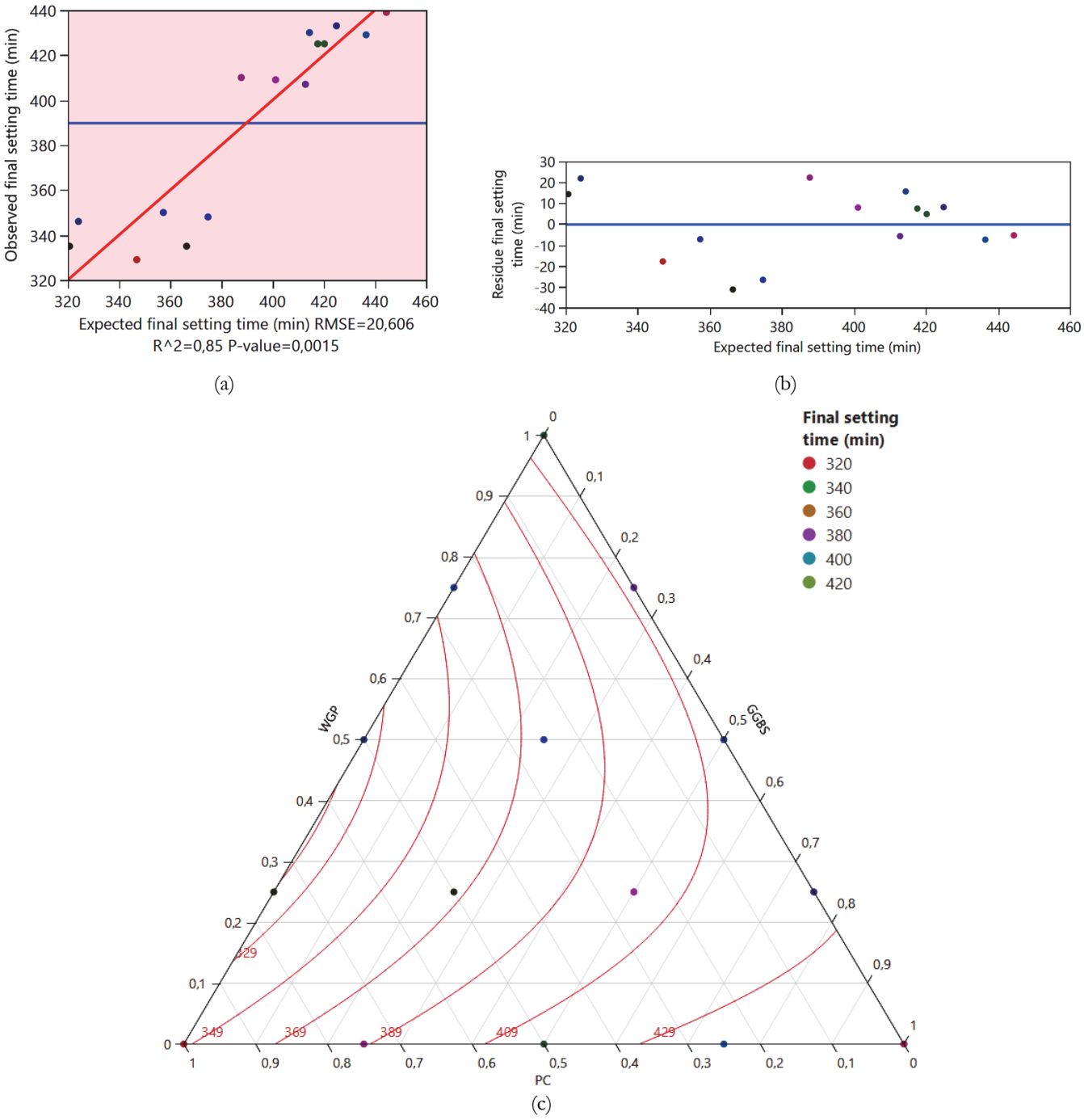

Figure 9: (a) Correlation curve between the observed (experimental) results and the expected results for final setting time; (b) Residue vs. expected final setting time; (c) Iso-response curve for final setting time.

Soundness

The soundness of cement refers to the stability of the volume change in the setting and hardening process. From Tab. 4, we can notice that the probability of the model, as expressed in eq.9, is close to 0, and the R^2 shows a relatively high correlation coefficient close to 1. These results indicate a good performance of the soundness model. The correlation curve between the observed results of soundness and the predicted results, as well as the graphical representation of residuals and the soundness iso-response curve, are shown in Figs. 10 (a),(b), and (c), respectively.

It can be noticed that the soundness of pastes is subordinate first by the increase in the dosage of GGBS, followed by the dosage of PC and WGP, then by the coupled effect of (WGP-GGBS), followed by (PC-WGP) and, finally, by the impact of (PC-GGBS). The test results for the soundness of pastes prepared in different proportions have shown an average value

of less than 10.0 mm before and after boiling, distance difference between the needle tip of the "Le-Chatelier apparatus" maximum specified by EN 169-3, showing that the agglomeration of the mixtures pastes has small and a constant volume change during the hardening process.

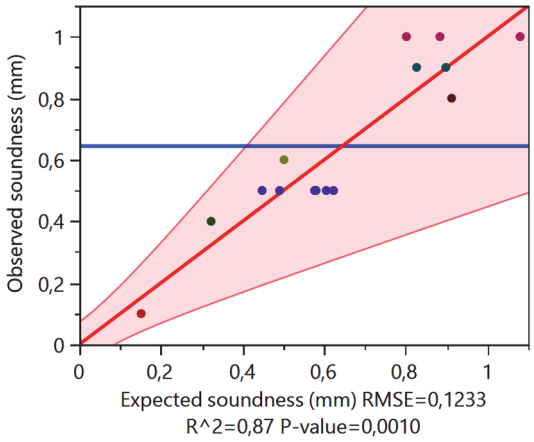

(a)

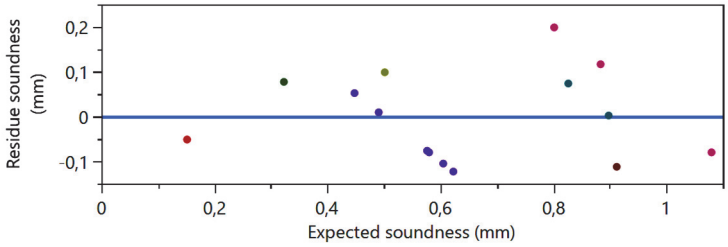

(b)

(a)

(b)

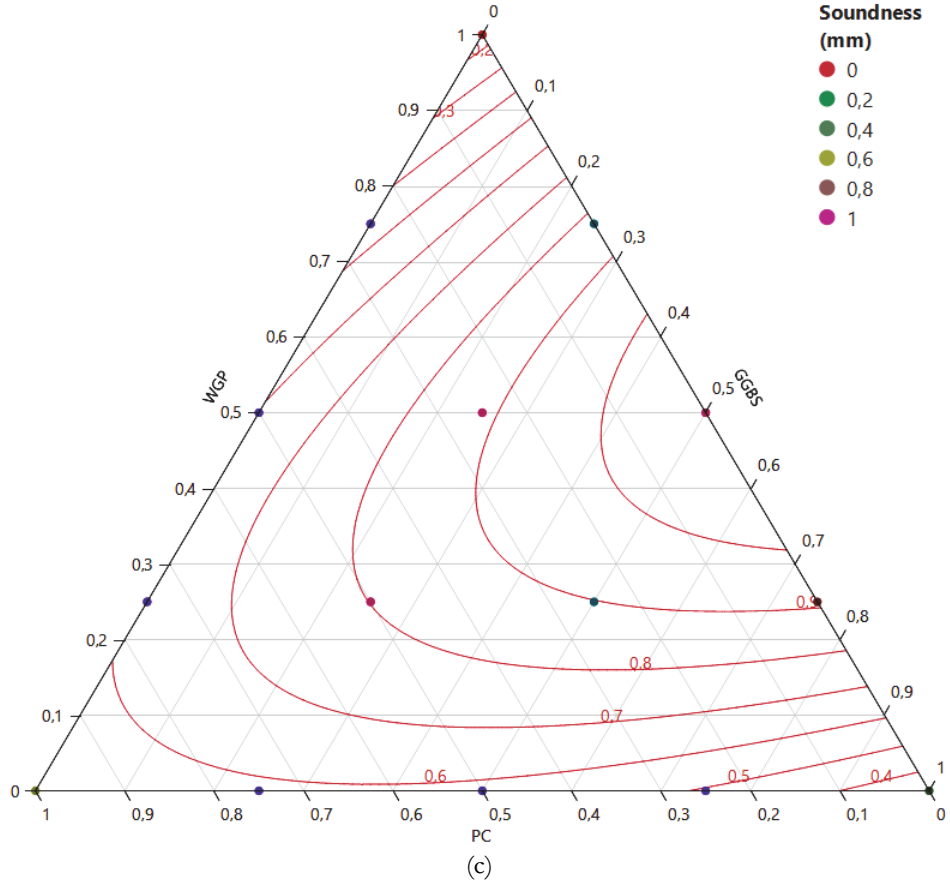

(c)

Figure 10: (a) Correlation curve between the observed (experimental) results and the expected results for soundness; (b) Residue vs. expected soundness; (c) Iso-response curve for soundness.

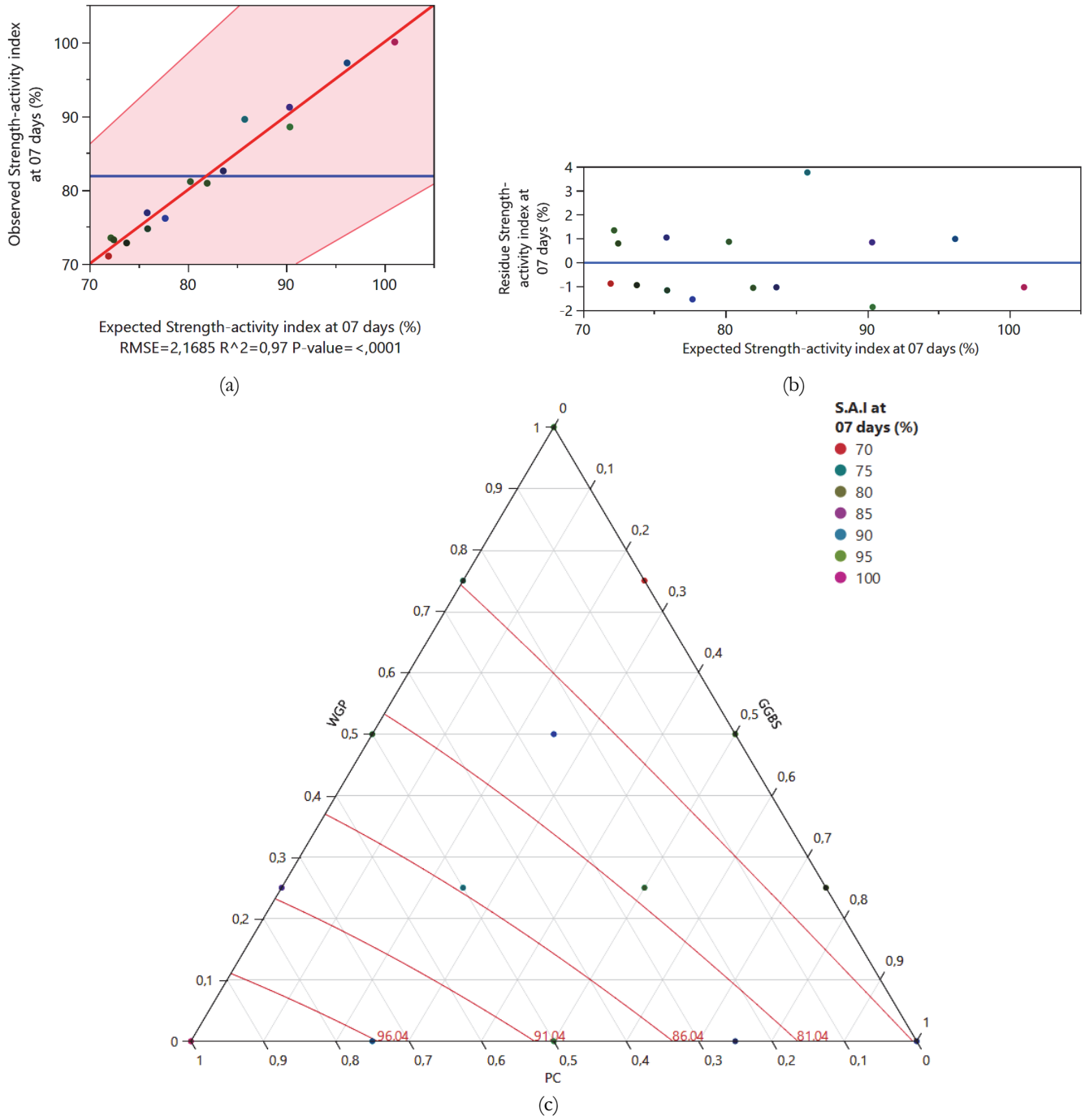

Figure 11: (a) Correlation curve between the observed (experimental) results and the expected results for SAI at 7 days; (b) Residue vs. expected SAI at 7 days; (c) Iso-response curve for SAI at 7 days.

Strength-activity index (S.A.I)

Strength-activity index experiments were conducted to evaluate the pozzolanic activity of WGP and GGBS on binary and ternary combinations and to investigate the synergistic impact of their use. The average compressive strengths for either 7 or 28 days of testing were measured to define the strength-activity index. Tab. 4 shows the 7-day and 28-day strength-activity index for binary and ternary mixes, including WGP and GGBS. As clearly indicated, the simulated models show a strong regression model with a significant correlation coefficient value of the correlation coefficients, i.e., R^2 = 0.97 and 0.92 for the 7-day and 28-day strength-activity index, respectively. Based on models for the 7-day and 28-day strength-activity index that have been predicted, it can be noted that the 7-day strength activity index is related initially by the PC content, followed

by the increase in the WGP and GGBS content and finally by the coupled effect of the (PC-GGBS). However, it was observed that the impact of the couple (PC-WGP) and (WGP-GGBS) caused a reduction in the strength-activity index. The results obtained for the 7 and 28-day strength-activity index are compared with the predicted responses given by the JMP16 software; they are represented graphically in Figs. 11 and 12, respectively. Based on Tab. 3, the 7-day strength-activity index of binary mixes, containing 5 %, 10 %, 15 %, and 20 % WGP, was 91.18 %, 80.9 %,74.74 %, and 73.51 %, respectively. The 7-day strength-activity index of binary mixes, including 5 % and 10 % GGBS, was 97.17 % and 88.51 %, respectively. However, at 15 % and 20 % dosage levels of GGBS, it was lower by 17.44 % and 23.10 %, respectively, compared with the control mortar.

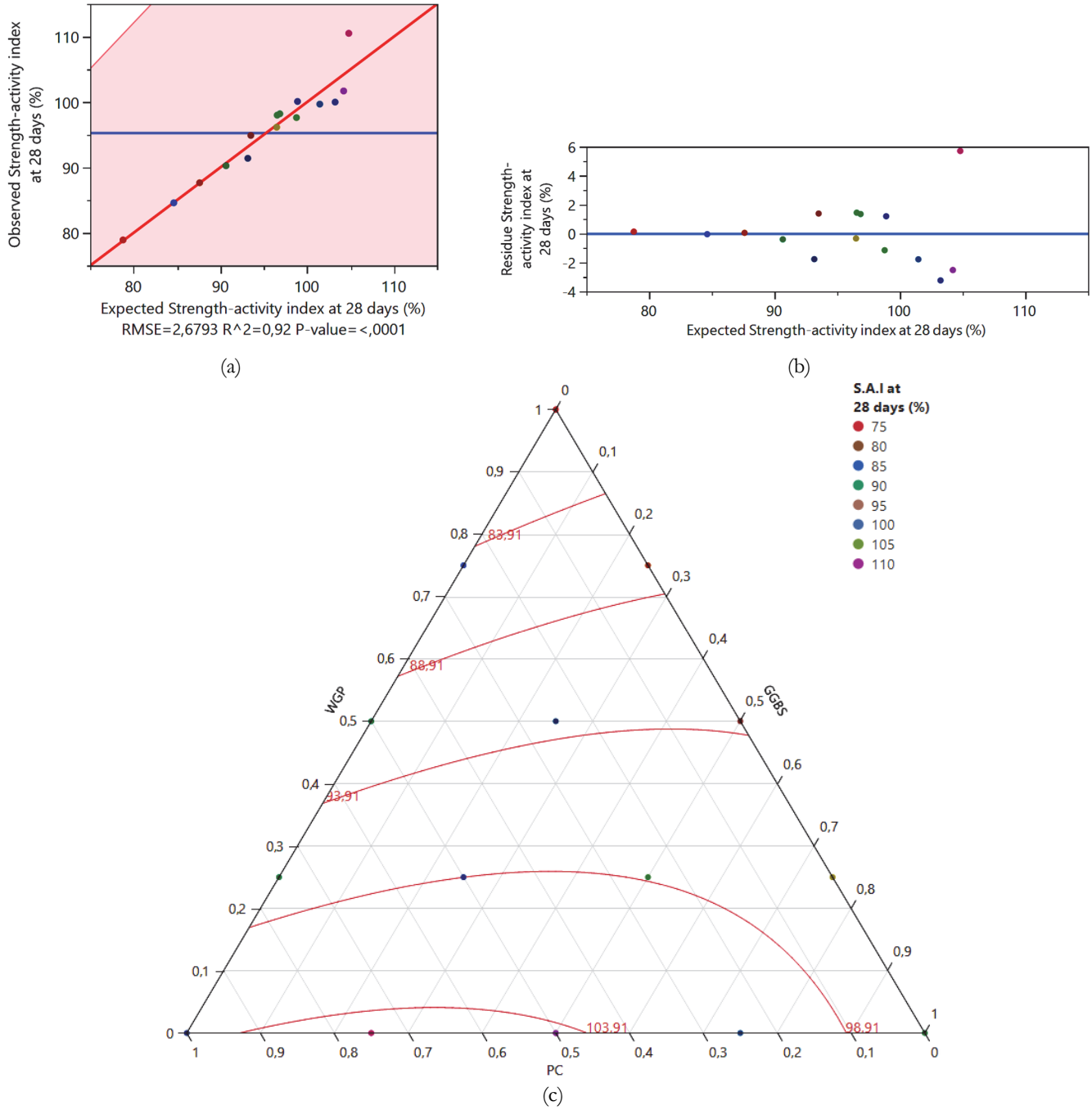

Figure 12: Correlation curve between the observed (experimental) results and the expected results for SAI at 28 days; (b) Residue vs. expected SAI at 28 days; (c) Iso-response curve for SAI at 28 days.

The relative 28-day strength-activity index of binary combinations, including 5 % GGBS, was 110.52 %. However, the 28-day strength-activity index at 15% and 20% dosage levels of GGBS were less than that of the reference mortar at 99.69% and 98%, respectively. According to Turkmen et al. [42], slag-blended concrete with lower GGBFS replacement proportions (of 10% to 30%) had the same or greater compressive strength than PC concrete after 28 days. Thus, Some researchers [43][44] also reported similar results when WGP was added to mortar mixtures with 20% as cement replacement, causing a decrease in compressive strength at 28 days compared to the control mix.

Even with increasing dosage levels of WGP, the strength-activity index values of the mortar samples containing WGP decreased gradually. The strength-activity index values of all mortar samples, including WGP, were above 75% (i.e., the minimum limit for the strength-activity index of supplementary cementitious materials at 28 days as required by the ASTM C618-12a). From these findings, it is clear that at reduced dosage levels of cement replacement (i.e., lower than 20% dosage), the GGBS shows a higher strength-activity index than WGP. However, with increasing dosage levels (i.e., 20%), GGBS performs better. Regarding ternary mixtures, it is evident that GGBS had a synergic impact when combined with WGP. This effect could significantly increase the compressive strength of the mortar samples, even at a low replacement level. The 28-day strength-activity index values of the mortar samples that contain blends of 5% of WGP and 5% of GGBS were 100.10 % by comparing the results of the strength-activity index of the mortar samples containing (5% WGP-10%GGBS) (i.e., 97.63 %) and (5% WGP-15%GGBS) (i.e., 96.16%). It is clear that by just replacing 5% of PC with GGBS, the strength-activity index decreased by 0.5%. When we used waste glass powder with four replacement rates, this synergic effect was also noted. According to the results of this study, it appears that by using WGP in combination with GGBS, not only WGP can be used as a valuable alternative Scms, but also the slower strength gain of GGBS mixtures can be considered.

It is worth mentioning that Elbahi et al.[34] have found that the incorporation of the couple (WGP–GGBS) in the ternary cement at a substitution rate of 20% at 28 days was similar to that of the control mortar. This behaviour may be due to the potential interaction between WGP and GGBS (synergistic effect).

Microstructural analysis using XRD and SEM-EDS techniques

In order to get a better understanding of the crystalline phase transition by the hydration process in cement, Cement-WGP, Cement-GGBS, and Cement-WGP-GGBS samples, the XRD patterns of these pastes are presented in Fig. 13. Quantitative XRD analyses were carried out on mixtures 01, 02, 06, 09, 12, and 14 at 28 days of curing. X'Pert High Score software was used to treat the obtained spectrograms. The XRD patterns revealed the presence of different phases, like ettringite, portlandite, quartz, hydrated calcium silicate, and calcite, which are the results of hydration reactions. The 2θ reflections at 18° are assigned to ettringite and portlandite, the hydration product of calcium aluminate minerals. The peaks observed in the reflection for ettringite and portlandite are less pronounced due to the consumption of portlandite by the pozzolanic hydration of slag. With an aluminosilicate polyhedron network in its vitreous body component, the slag is a supplement cementitious material rich in aluminium. The aluminate ions from the aluminosilicate network, which are involved in cement hydration, depolymerise when slag is activated in cement paste. Excess Al_2O_3 reacts with SO_3 to form monosulfate because the formation of ettringite requires three parts Al_2O_3 and one part SO_3 [45]. Ettringite and portlandite can form in some cementitious materials, including WGP-GGBS pastes, under the right temperature, pH, and specific ions. Hydrated calcium silicate, also known as calcium silicate hydrate (C-S-H), is a key component of many cementitious materials, including WGP-GGBS pastes. C-S-H forms when calcium ions from the slag react with silicate ions from the glass under conditions that promote the formation of this mineral. As the C-S-H gel like substance hardens, it provides the material's binding strength and durability, helping it to resist cracking, deformation, and other forms of damage. This makes C-S-H a key contributor to slag-glass pastes' overall properties and performance. It should also be noted that the calcite and quartz peaks were proportional to the waste glass powder (WGP) and ground granulated blast furnace slag (GGBS) contents. In addition, the formation of calcite, a form of calcium carbonate, in a WGP-GGBS paste will depend on several factors, including the composition of the original glass used in the paste, the amount of calcium and carbonate ions, the pH and temperature of the mixture.

According to XRD, SEM, and EDS analyses, the same paste samples were examined to investigate the effect of WGP and GGBS on the microstructural characteristics of PC pastes with varying replacement proportions. The obtained results are illustrated in Figs. 14a, 15a, 16a, 17a, 18a, and 19a. The SEM images were captured at a scale of 10 μm (5000x), allowing for the observation of the main phases of hydrated cement. These observations, combined with EDS analysis, facilitated the identification of the main structures and hydrates present in the cement matrix of each formulation.

In Fig. 14a, it can be observed that CH (calcium hydroxide) dominated in the PC paste without SCMs after a curing time of 28 days. Figs. 14a and 15a demonstrate that both PC and WGP particles exhibit irregular shapes with sharp edges and glassy structures. The addition of WGP to the PC paste specimen resulted in the formation of a Si-rich layer on the surface of the WGP particle due to its incongruent dissolution. This layer reacted with Ca to form the C–S–H reaction rim, as shown in

Fig. 15a. Fig. 16 presents SEM micrographs of the fracture surface of hardened paste samples containing 7.5% GGBS as a cement replacement after 28 days of hydration. The specimen is predominantly composed of GGBS particles, identifiable by their bright grey tone and sharp irregular morphology. Numerous partly reacted and unreacted GGBS particles can be observed. This microstructure exhibits disconnected pores with limited CSH (calcium silicate hydrate) around the GGBS particles, resulting in a dark tone. The SEM images of mixtures N° 09, 12, and 14 reveal that the cementitious matrix of the hardened paste samples, which include SCMs as cement replacement, is denser than the control specimen. This evidence is presented in Figs. 17, 18, and 19, which clearly show a significantly lower degree of pore space (dark area) compared to the control (depicted in Fig. 14). At a curing age of 28 days, the reduced degree of pore space in WGP22.5GGBS7.5, WGP15GGBS15, and WGP7.5GGBS22.5 contributes to improved strength properties when compared to the control specimen. By participating in small amounts in the hydration reaction or acting as a fine aggregate in the blended cementitious material, WGP can contribute to early curing. However, GGBS has been found to inhibit PC hydration in its early stages. The addition of GGBS hinders the nucleation and growth of C–S–H by increasing the concentration of Ca in the pore solution and reducing the supersaturation relative to CH. However, the early contribution of WGP is more significant than that of GGBS when added to a cement-based material containing GGBS. This condition accounts for the dense micromorphology of the blend prepared through the synergistic replacement of partial PC by WGP and GGBS. In general, the different specimens exhibit a compact microstructure.

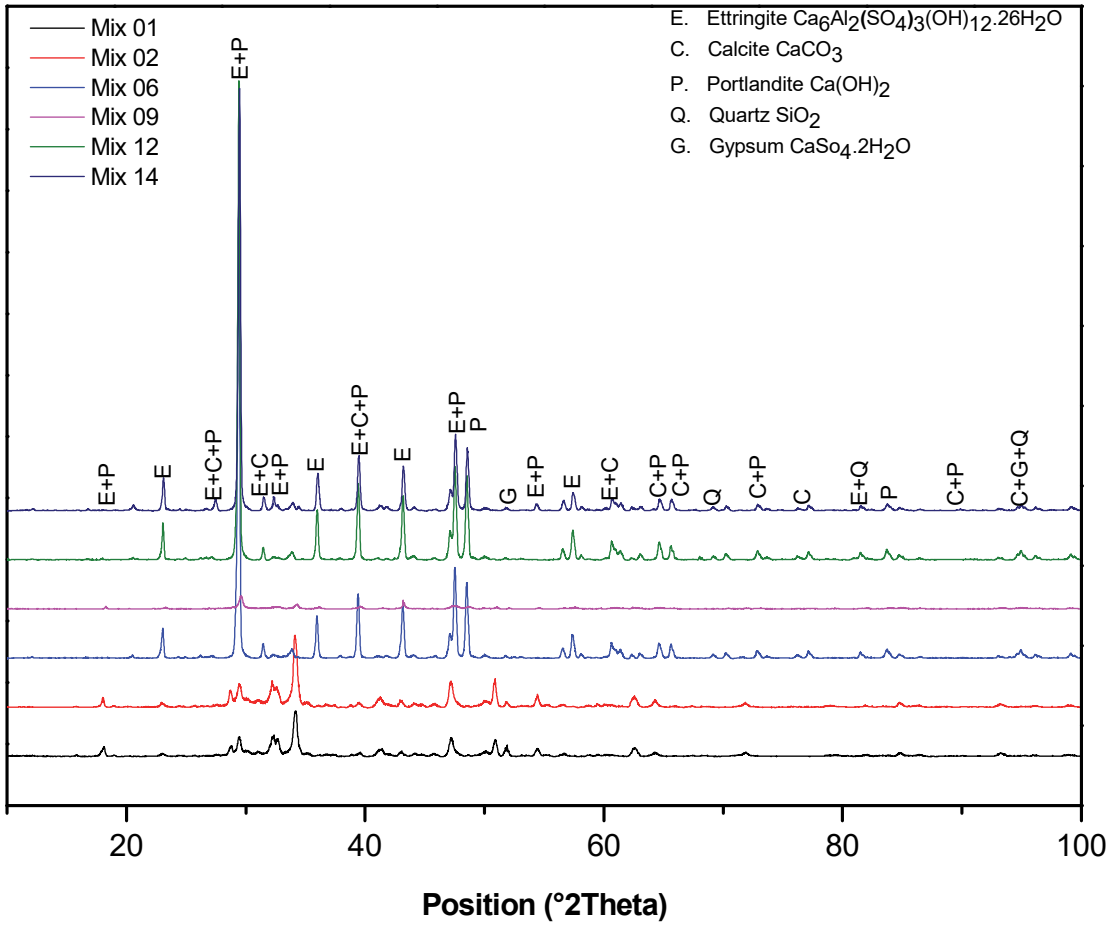

Figure 13: XRD spectrogram of hardened paste samples (Mix 01,02,06,09,12 and 14)

The formation of brucite ($Mg(OH)_2$) in the samples, observed by SEM as hexagonal plate-shaped crystals often agglomerated in spherical morphology, was not found in the SEM images. Therefore, no brucite was apparent in the SEM analyses of samples containing GGBS or WGP in binary and ternary mixtures. This observation is consistent with the XRD results, which also showed no brucite formation in the powder specimens. As shown in Figs. 14b, 15b, 16b, 17b, 18b, and 19b, EDS analysis indicated the presence of mainly Si, Ca, O, and Mg in the different hardened paste samples. These components correspond to the formation of C-S-H (calcium silicate hydrate) or the amorphous silica of GGBS and WGP, which actively participated in the pozzolanic reaction to enhance strength development.

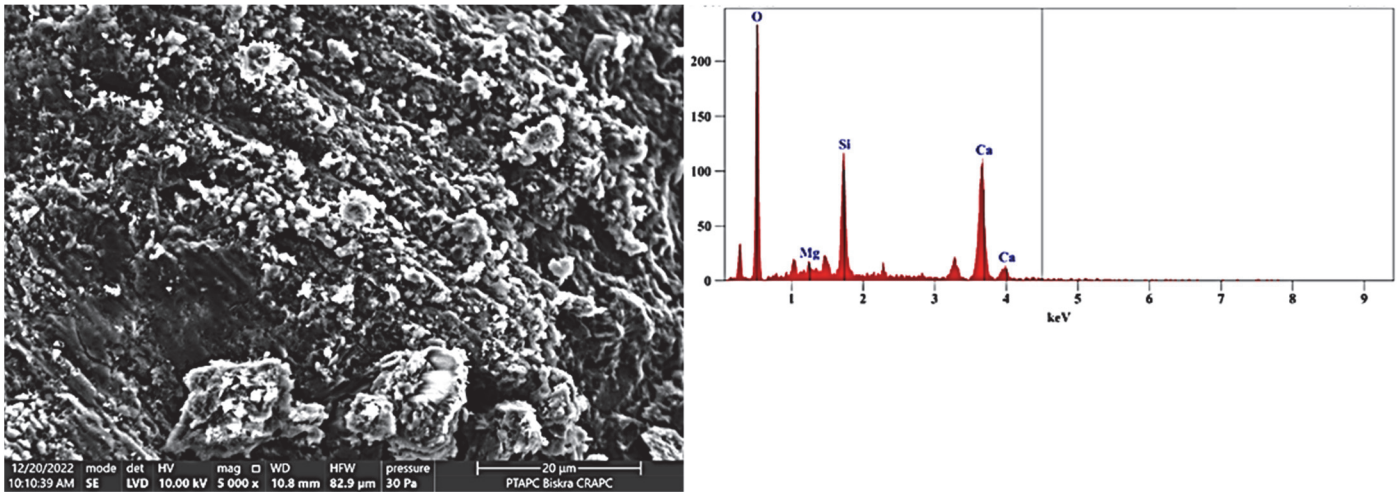

(a) (b)

Figure 14: SEM (a) and EDS (b) of hardened paste samples (control mixture) without Scms (Mix 01).

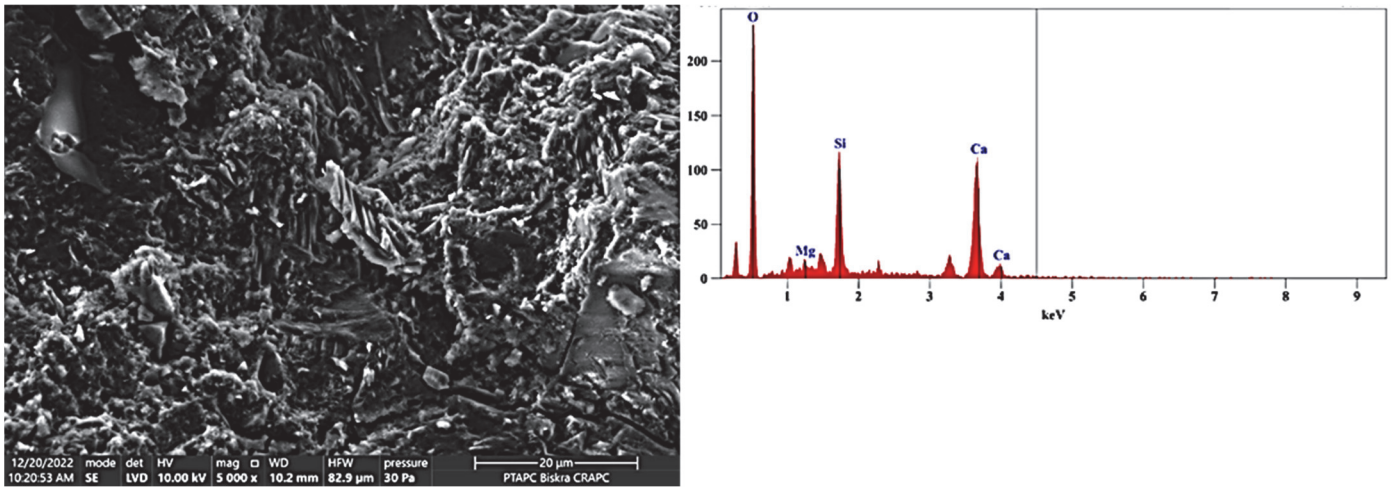

(a) (b)

Figure 15: SEM (a) and EDS (b) of hardened paste samples containing 7.5% WGP as cement replacement (Mix 02).

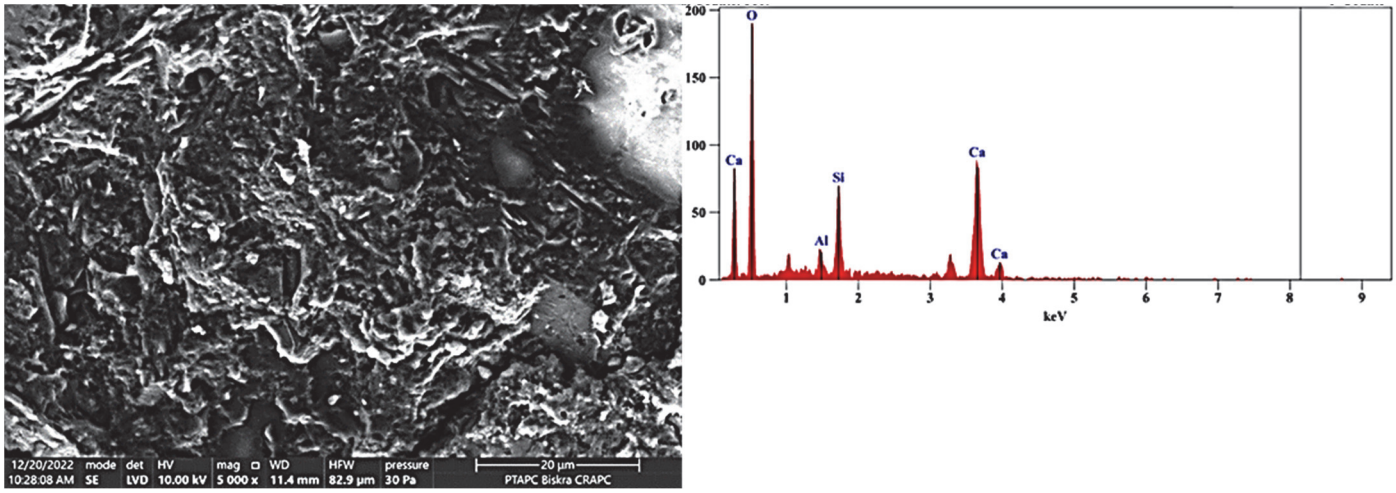

(a) (b)

Figure 16: SEM (a) and EDS (b) of hardened paste samples containing 7.5% GGBS as cement replacement (Mix 06).

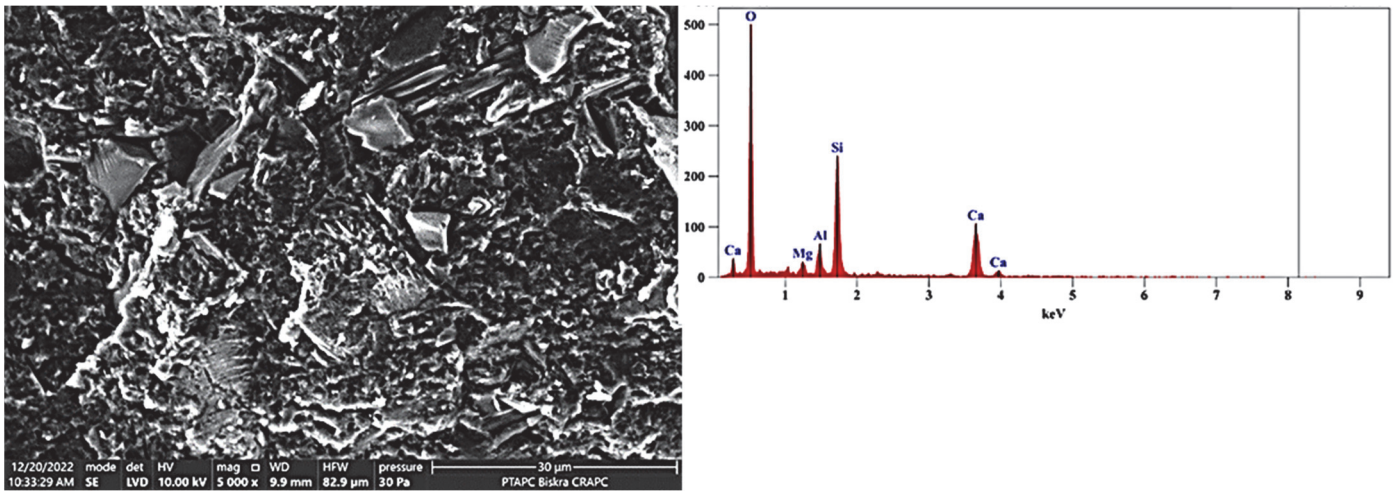

(a) (b)

Figure 17: SEM (a) and EDS (b) of hardened paste samples containing 22.5% WGP and 7.5% GGBS as cement replacement (Mix 09).

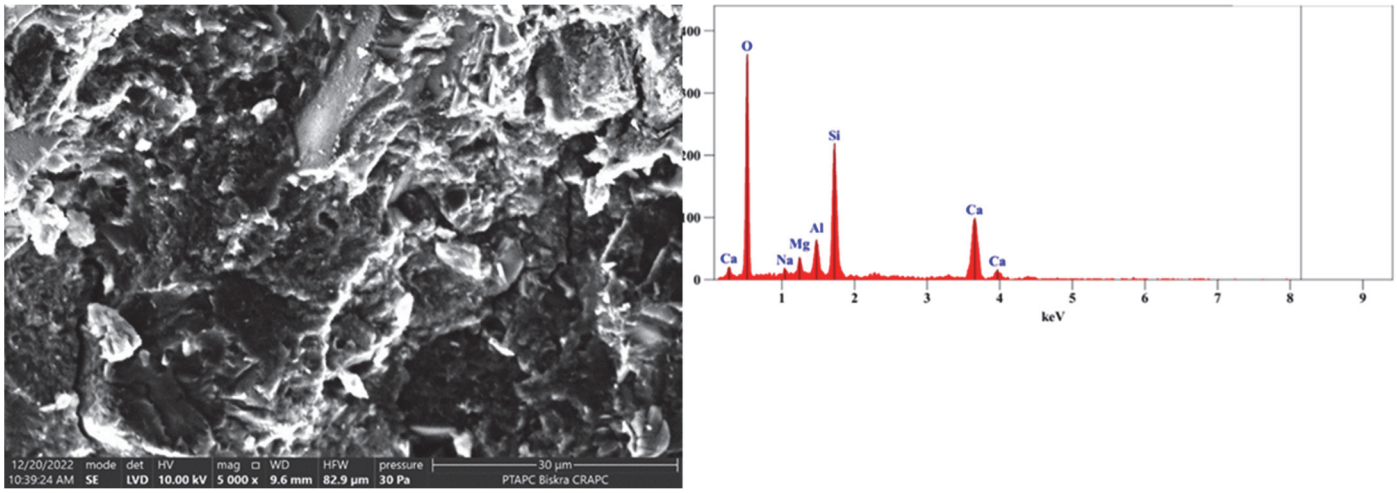

(a) (b)

Figure 18: SEM (a) and EDS (b) of hardened paste samples containing 15% WGP and 15% GGBS as cement replacement (Mix 12).

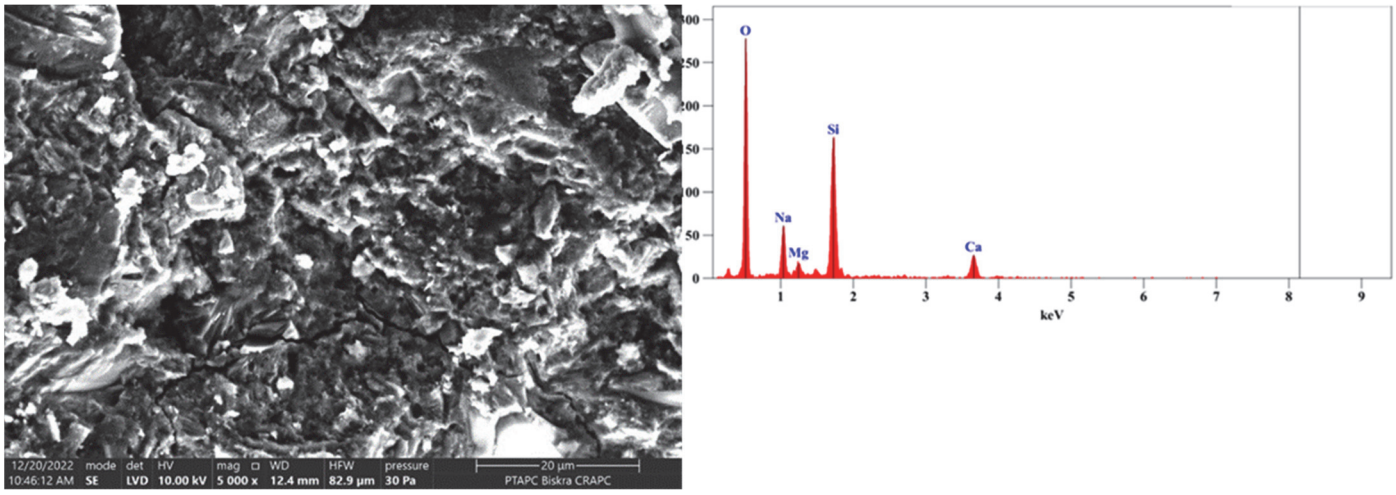

(a) (b)

Figure 19: SEM (a) and EDS (b) of hardened paste samples containing 7.5% WGP and 22.5% GGBS as cement replacement (Mix 14).

Conclusion

In this study, an experimental investigation was conducted to study the influence of waste glass powder (WGP) and ground granulated blast furnace slag (GGBS) as supplementary cementitious materials (SCMs). Analyses of fresh, mechanical, and microstructural properties were performed. The following conclusions can be drawn from the results obtained:

- The mixture design approach allowed for precise mathematical models and prediction values of consistency, setting time, strength, and resistance activity index of the examined pastes and mortars.
- Incorporating 7.5% WGP and 7.5% GGBS in the cement reduced water requirements by 0.5% and 0.6% to achieve a normal paste consistency. Furthermore, the addition of 22.5% GGBS in ternary binders resulted in an additional improvement of approximately 3.4% in consistency.
- WGP and GGBS-based mixes exhibited longer initial and final setting times in accordance with ASTM C150 standards.
- Partial cement replacement with WGP up to 20% led to a 21% decrease in the strength activity index at 28 days compared to the reference mortar. Similarly, replacing 20% of the binder with GGBS achieved a maximum strength of 47.5 MPa, corresponding to a 2% reduction in the strength activity index.
- Incorporating 5% WGP and 5% GGBS in ternary binders significantly reduced the total porosity of the samples, promoting a compressive strength of 48.5 MPa at 28 days, compared to the 48.47 MPa of the control mix.
- The results of the strength activity index exceeded 75% at 7 and 28 days, indicating positive pozzolanic activity of WGP and GGBS when replacing cement.
- X-ray diffraction (XRD), scanning electron microscopy (SEM), and energy-dispersive spectroscopy (EDS) analyses revealed that the hydration process resulted in the formation of additional calcium silicate hydrate (C-S-H) gel, contributing to the strength and durability of the paste.

This study provides valuable insights into the potential use of recycled materials in construction and can contribute to promoting the transition towards a more sustainable and environmentally friendly building industry.

Nomenclature

PC: Portland Cement
SCMs: Supplementary Cementitious materials
GGBS: Ground Granulated Blast Furnace Slag
WGP: Waste Glass Powder
(W/C): (Water / Cement) ratio
7-days SAI: Strength-Activity Index at 7 days
28-days SAI: Strength-Activity Index at 28 days

Acknowledgements

The authors would like to acknowledge the directorate general for scientific research and technological development "DGRSDT" -Algeria- for financial support, and the performance directorate of the Biskria cement company where this work was conducted for their technical support.

References

[1] Laoufi, L., Senhadji, Y., Benazzouk, A. (2016). Valorization of mud from Fergoug dam in manufacturing mortars, Case Stud. Constr. Mater., 5, pp. 26–38, DOI: 10.1016/j.cscm.2016.06.002.

[2] Al-Mansour, A., Chow, C.L., Feo, L., Penna, R., Lau, D. (2019). Green concrete: By-products utilization and advanced approaches, Sustain., 11(19), pp. 1–30, DOI: 10.3390/su11195145.

[3] Zhang, J., Liu, G., Chen, B., Song, D., Qi, J., Liu, X. (2014). Analysis of CO2 Emission for the Cement Manufacturing with Alternative Raw Materials: A LCA-based Framework, Energy Procedia, 61, pp. 2541–2545, DOI: 10.1016/j.egypro.2014.12.041.
[4] Shubbar, A.A., Nasr, M.S., Islam, G.M.S., Al-Khafaji, Z.S., Sadique, M., Hashim, K., Assi, L.N. (2022). Early Age and Long-term Mechanical Performance of Mortars Incorporating High-volume GGBS, vol. 184, Springer Singapore.
[5] Xu, A., Sarkar, S.L., Nilsson, L.O. (1993). Effect of fly ash on the microstructure of cement mortar, Mater. Struct., 26(7), pp. 414–424, DOI: 10.1007/BF02472942.
[6] Pourabbas Bilondi, M., Toufigh, M.M., Toufigh, V. (2018). Experimental investigation of using a recycled glass powder-based geopolymer to improve the mechanical behavior of clay soils, Constr. Build. Mater., 170, pp. 302–313, DOI: 10.1016/j.conbuildmat.2018.03.049.
[7] Belkadi, A.A., Kessal, O., Chiker, T., Achour, Y., Rouabhi, A., Messaoudi, O., Khouadjia, M.L.K. (2022). Full Factorial Design of Mechanical and Physical Properties of Eco-mortars Containing Waste Marble Powder, Arab. J. Sci. Eng., DOI: 10.1007/s13369-022-06971-7.
[8] Soltaninejad, M., Soltaninejad, M., Farshad Saberi, K., Moshizi, M.K., Sadeghi, V., Jahanbakhsh, P. (2021). Environmental-friendly mortar produced with treated and untreated coal wastes as cement replacement materials, Clean Technol. Environ. Policy, 23(10), pp. 2843–2860, DOI: 10.1007/s10098-021-02204-x.
[9] Virgalitte, S.J., Luther, M.D., Rose, J.H., Mather, B., Bell, L.W., Ehmke, B.A., Klieger, P., Roy, D.M., Call, B.M., Hooton, R.D. (1995). Ground Granulated blast-furnace slag as a cementitious constituent in concrete, Am. Concr. Inst. ACI Rep. 233R-95.
[10] Logbi, A., Kriker, A., Snisna, Z. (2017). Effects of mineral additions on durability and physico-mechanical properties of mortar, AIP Conf. Proc., 1814, DOI: 10.1063/1.4976251.
[11] Melais, F.Z., Achoura, D., Ghorbel, E. (2022). Durability of mortars containing blast furnace slags used as a partial substitute of Portland cement exposed to external sulfate attacks Durability of mortars containing blast furnace slags used as a partial substitute of Portland cement exposed to extern, J. Mater. Environ. Sci., 12(6), pp. 837–852.
[12] Crossin, E. (2015). The greenhouse gas implications of using ground granulated blast furnace slag as a cement substitute, J. Clean. Prod., 95, pp. 101–118, DOI: 10.1016/j.jclepro.2015.02.082.
[13] Mounanga, P., Khokhar, M.I.A., El Hachem, R., Loukili, A. (2011). Improvement of the early-age reactivity of fly ash and blast furnace slag cementitious systems using limestone filler, Mater. Struct., 44(2), pp. 437–453, DOI: 10.1617/s11527-010-9637-1.
[14] Gruyaert, E., Robeyst, N., De Belie, N. (2010). Study of the hydration of Portland cement blended with blast-furnace slag by calorimetry and thermogravimetry, J. Therm. Anal. Calorim., 102(3), pp. 941–951, DOI: 10.1007/s10973-010-0841-6.
[15] Jiang, W., Silsbee, M.R., Roy, D.M. (1997). Similarities and differences of microstructure and macro properties between portland and blended cement, Cem. Concr. Res., 27(10), pp. 1501–1511, DOI: 10.1016/S0008-8846(97)00169-5.
[16] Hooton, R.D. (2000). Canadian use of ground granulated blast-furnace slag as a supplementary cementing material for enhanced performance of concrete, Can. J. Civ. Eng., 27(4), pp. 754–760, DOI: 10.1139/cjce-27-4-754.
[17] Sajedi, F. (2012). Mechanical activation of cement–slag mortars, Constr. Build. Mater., 26(1), pp. 41–48, DOI: 10.1016/j.conbuildmat.2011.05.001.
[18] Rahman, M.A., Sarker, P.K., Shaikh, F.U.A., Saha, A.K. (2017). Soundness and compressive strength of Portland cement blended with ground granulated ferronickel slag, Constr. Build. Mater., 140, pp. 194–202, DOI: 10.1016/j.conbuildmat.2017.02.023.
[19] Belebchouche, C., Moussaceb, K., Bensebti, S.E., Aït-Mokhtar, A., Hammoudi, A., Czarnecki, S. (2021). Mechanical and microstructural properties of ordinary concrete with high additions of crushed glass, Materials (Basel), 14(8), DOI: 10.3390/ma14081872.
[20] Islam, G.M.S., Rahman, M.H., Kazi, N. (2017). Waste glass powder as partial replacement of cement for sustainable concrete practice, Int. J. Sustain. Built Environ., 6(1), pp. 37–44, DOI: 10.1016/j.ijsbe.2016.10.005.
[21] Aliabdo, A.A., Abd Elmoaty, A.E.M., Aboshama, A.Y. (2016). Utilization of waste glass powder in the production of cement and concrete, Constr. Build. Mater., 124, pp. 866–877, DOI: 10.1016/j.conbuildmat.2016.08.016.
[22] Khan, F.A., Shahzada, K., Ullah, Q.S., Fahim, M., Khan, S.W., Badrashi, Y.I. (2020). Development of environment-friendly concrete through partial addition of waste glass powder (Wgp) as cement replacement, Civ. Eng. J., 6(12), pp. 2332–2343, DOI: 10.28991/cej-2020-03091620.
[23] Yannick, T.L., Luc Leroy, M.N., Liliane Van Essa, K.S., Arlin Bruno, T., Ismaïla, N., Thomas, A.B. (2020). Mechanical and microstructural properties of Cameroonian CPJ NC CEM II/B-P 42.5R cement substitution by glass powder in the cement paste and mortar, SN Appl. Sci., 2(8), pp. 1–12, DOI: 10.1007/s42452-020-3152-y.

[24] Jiang, X., Xiao, R., Bai, Y., Huang, B., Ma, Y. (2022). Influence of waste glass powder as a supplementary cementitious material (SCM) on physical and mechanical properties of cement paste under high temperatures, J. Clean. Prod., 340(December 2021), pp. 130778, DOI: 10.1016/j.jclepro.2022.130778.
[25] Matos, A.M., Sousa-Coutinho, J. (2012). Durability of mortar using waste glass powder as cement replacement, Constr. Build. Mater., 36, pp. 205–215, DOI: 10.1016/j.conbuildmat.2012.04.027.
[26] Xuan, M.Y., Han, Y., Wang, X.Y. (2021). The hydration, mechanical, autogenous shrinkage, durability, and sustainability properties of cement–limestone–slag ternary composites, Sustain., 13(4), pp. 1–21, DOI: 10.3390/su13041881.
[27] Van Tuan, N., Ye, G., van Breugel, K., Fraaij, A.L.A., Bui, D.D. (2011). The study of using rice husk ash to produce ultra high performance concrete, Constr. Build. Mater., 25(4), pp. 2030–2035, DOI: 10.1016/j.conbuildmat.2010.11.046.
[28] Wan, S., Zhou, X., Zhou, M., Han, Y., Chen, Y., Geng, J., Wang, T., Xu, S., Qiu, Z., Hou, H. (2018). Hydration characteristics and modeling of ternary system of municipal solid wastes incineration fly ash-blast furnace slag-cement, Constr. Build. Mater., 180, pp. 154–166, DOI: 10.1016/j.conbuildmat.2018.05.277.
[29] Deboucha, W., Leklou, N., Khelidj, A. (2022). Combination effect of limestone filler and slag on hydration reactions in ternary cements, Eur. J. Environ. Civ. Eng., 26(9), pp. 3931–3946, DOI: 10.1080/19648189.2020.1825233.
[30] Han, Y., Oh, S., Wang, X.-Y., Lin, R.-S. (2021). Hydration–Strength–Workability–Durability of Binary, Ternary, and Quaternary Composite Pastes, Materials (Basel)., 15(1), pp. 204, DOI: 10.3390/ma15010204.
[31] Makhloufi, Z., Aggoun, S., Benabed, B., Kadri, E.H., Bederina, M. (2016). Effect of magnesium sulfate on the durability of limestone mortars based on quaternary blended cements, Cem. Concr. Compos., 65, pp. 186–199, DOI: 10.1016/j.cemconcomp.2015.10.020.
[32] Dave, N., Misra, A.K., Srivastava, A., Sharma, A.K., Kaushik, S.K. (2017). Study on quaternary concrete micro-structure, strength, durability considering the influence of multi-factors, Constr. Build. Mater., 139, pp. 447–457, DOI: 10.1016/j.conbuildmat.2017.02.068.
[33] Liu, G., Florea, M.V.A., Brouwers, H.J.H. (2019). Characterization and performance of high volume recycled waste glass and ground granulated blast furnace slag or fly ash blended mortars, J. Clean. Prod., 235, pp. 461–472, DOI: 10.1016/j.jclepro.2019.06.334.
[34] Elbahi, B.S., Zeghichi, L. (2022). Durability aspects and mechanical strength of mortars containing glass powder and slag, Adv. Cem. Res., 34(5), pp. 197–205, DOI: 10.1680/jadcr.20.00064.
[35] Ramakrishnan, K., Pugazhmani, G., Sripragadeesh, R., Muthu, D., Venkatasubramanian, C. (2017). Experimental study on the mechanical and durability properties of concrete with waste glass powder and ground granulated blast furnace slag as supplementary cementitious materials, Constr. Build. Mater., 156, pp. 739–749, DOI: 10.1016/j.conbuildmat.2017.08.183.
[36] Goupy, J., Creighton, L. (2007). Introduction to design of experiments with JMP examples, SAS publishing.
[37] Zaitri, R., Bederina, M., Bouziani, T., Makhloufi, Z., Hadjoudja, M. (2014). Development of high performances concrete based on the addition of grinded dune sand and limestone rock using the mixture design modelling approach, Constr. Build. Mater., 60, pp. 8–16, DOI: 10.1016/j.conbuildmat.2014.02.062.
[38] Boudina, T., Benamara, D., Zaitri, R. (2021). Optimization of high-performance-concrete properties containing fine recycled aggregates using mixture design modeling, Frat. Ed Integrita Strutt., 15(57), pp. 50–62, DOI: 10.3221/IGF-ESIS.57.05.
[39] [39] He, X., Ma, M., Su, Y., Lan, M., Zheng, Z., Wang, T., Strnadel, B., Zeng, S. (2018). The effect of ultrahigh volume ultrafine blast furnace slag on the properties of cement pastes, Constr. Build. Mater., 189, pp. 438–447, DOI: 10.1016/j.conbuildmat.2018.09.004.
[40] Yingliang, Z., Jingping, Q., Zhengyu, M.A., Zhenbang, G., Hui, L. (2020). Effect of superfine blast furnace slags on the binary cement containing high-volume fly ash, Powder Technol., 375, pp. 539–548, DOI: 10.1016/j.powtec.2020.07.094.
[41] Heikal, M., Abd El Aleem, S., Morsi, W.M. (2013). Characteristics of blended cements containing nano-silica, HBRC J., 9(3), pp. 243–255, DOI: 10.1016/j.hbrcj.2013.09.001.
[42] Türkmen, I., Öz, A., Aydin, A.C. (2010). Characteristics of workability, strength, and ultrasonic pulse velocity of SCC containing zeolite and slag, Sci. Res. Essays, 5(15), pp. 2055–2064.
[43] Shi, C., Wu, Y., Riefler, C., Wang, H. (2005). Characteristics and pozzolanic reactivity of glass powders, Cem. Concr. Res., 35(5), pp. 987–993, DOI: 10.1016/j.cemconres.2004.05.015.
[44] Šimonová, H., Zahálková, J., Rovnaníková, P., Bayer, P., Keršner, Z., Schmid, P. (2017). Mechanical Fracture Parameters of Cement Based Mortars with Waste Glass Powder, Procedia Eng., 190, pp. 86–91, DOI: 10.1016/j.proeng.2017.05.311.

[45] Yang, J., Ding, Q., Zhang, G., Hou, D., Zhao, M., Cao, J. (2022). Effect of sulfate attack on the composition and micro-mechanical properties of C-A-S-H gel in cement-slag paste: A combined study of nanoindentation and SEM-EDS, Constr. Build. Mater., 345, pp. 128275, DOI: 10.1016/j.conbuildmat.2022.128275.